Journal of Inflammation Research

Dovepress
open access to scientific and medical research

Open Access Full Text Article

ORIGINAL RESEARCH

NLRP3 Inflammasome Inhibition After Pilocarpine-Induced Status Epilepticus Attenuates Chronic Inflammation in Epileptic Mice

Lei Wang[1,*], Kai Wang[2,*], Yuwen Chen[1], Xiaoyu Zhang[1,3], Wenhao Xu[1,3], Zhong Dong[1,3], Yu Wang[1,3,4]

[1]Department of Neurology, The First Affiliated Hospital of Anhui Medical University, Hefei, Anhui Province, 230000, People's Republic of China; [2]Department of Neurology, The Third Affiliated Hospital of Anhui Medical University, Hefei, Anhui Province, 230000, People's Republic of China; [3]Department of Neurology, Anhui Public Health Clinical Center, Hefei, Anhui Province, 230000, People's Republic of China; [4]Department of Neurology, Anqing First People's Hospital Affiliated to Anhui Medical University, Anqing, Anhui Province, 246000, People's Republic of China

*These authors contributed equally to this work

Correspondence: Yu Wang, Department of Neurology, The First Affiliated Hospital of Anhui Medical University, Hefei, Anhui Province, 230000, People's Republic of China, Email yw4d@hotmail.com

Objective: To investigate the effects of inhibiting the NOD-like receptor family pyrin domain-containing 3 (NLRP3) inflammasome on neuronal damage and chronic pro-inflammatory responses during epileptogenesis in a mouse model of pilocarpine-induced status epilepticus (SE).

Methods: Mice were randomly allocated into three groups: control, SE, and SE + MCC 950. The expression patterns of M1 and M2 microglial biomarkers in the hippocampus were quantified using Western blotting, quantitative real-time polymerase chain reaction, enzyme-linked immunosorbent assay, and immunofluorescence staining. Additionally, seizure susceptibility, video-electroencephalography recording, Morris water maze test, and brain immunofluorescence staining were performed to evaluate the epileptic brain 4 weeks post-SE.

Results: Within 72 hours post-SE, hippocampal microglia demonstrated a preferential polarization towards the M1 phenotype, a trend that was mitigated by NLRP3 inflammasome inhibition. During epileptogenesis, SE mice treated with NLRP3 inflammasome inhibition exhibited reduced neuronal damage, improved cognitive function, decreased seizure susceptibility, and attenuated chronic pro-inflammatory responses.

Conclusion: Inhibition of NLRP3 inflammasome post-SE effectively ameliorates neuronal loss, seizure susceptibility, and cognitive dysfunction during epileptogenesis. This neuroprotective effect may be mediated through the mitigation of chronic pro-inflammatory responses within the epileptic brain.

Keywords: NLRP3 inflammasome, microglial polarization, M1 microglia, epileptogenesis, chronic pro-inflammatory response

Introduction

Epilepsy, an abnormal brain condition characterized by an enduring predisposition to spontaneous epileptic seizures, affects over 70 million people globally.[1] Several diseases such as depression, anxiety, migraine, and sleep disorder, are more common in people with epilepsy than in the general population.[2] Despite progress in the development of antiseizure medications (ASMs), approximately 30–40% of epileptic patients develop drug-resistance,[2,3] which is contributed to ASMs primarily suppress seizures rather than addressing the underlying pathological conditions.[4] These pathological alterations, including altered gene expression, dysregulated protein production, disrupted neuronal connectivity, and inflammation, are thought to drive epileptogenesis.[2,5–9]

It has been accepted that inflammation plays a role in transforming a normal neuronal network into an epileptic brain.[1,10–13] Activated microglia and elevated pro-inflammatory cytokines have been observed in epileptic brains.[6–9,12]

Received: 18 March 2024
Accepted: 22 August 2024
Published: 7 September 2024

Generally, activated microglia are condensed into the phenotypes of M1 (pro-inflammatory) and M2 (anti-inflammatory) .[14] In a KA-induced epileptic model, upregulation of M1 microglial biomarkers following status epilepticus (SE) was associated with increased seizure frequency during epileptogenesis.[11] Postnatal febrile seizures induced by IL-1β increase seizure susceptibility in adulthood, which can be prevented by IL-1β receptor antagonist.[15] Notably, IL-10, an anti-inflammatory cytokine secreted by M2 microglia, downregulates IL-1β in the brain subjected to an epileptogenic injury.[16,17] These results suggest that the modulation of microglial polarization plays a potential role in restraining epileptogenesis.

The NOD-like receptor family pyrin domain-containing 3 (NLRP3) inflammasome is composed of NLRP3, apoptosis-associated speck-like protein (ASC), and effector protein Caspase-1,[18] functions to catalyze pro-IL-1β and pro-IL-18 into mature IL-1β and IL-18, respectively.[19] Previous studies have reported that the NRLP3 inflammasome is highly expressed in microglia located within epileptogenic foci.[20,21] Suppressed expression of the NLRP3 inflammasome exhibits neuroprotective effects by alleviating the pro-inflammatory response.[22] In addition, IL-10 decreases the levels of IL-1β by inhibiting NLRP3 inflammasome activation.[16] These findings underscore the potential of inhibiting the NLRP3 inflammasome in modulating M1 microglial polarization.

However, the influence of NLRP3 inflammasome inhibition post-SE on microglial polarization and the subsequent inflammatory response in the epileptic brain have not been explored. In the present study, we inhibited the NLRP3 inflammasome through pretreatment with MCC950 (a specific inhibitor of NLRP3), finding a significant reduction in the levels of biomarkers associated with M1 microglia in the hippocampi of pilocarpine-induced SE mice. Decreased neuronal damage and improved seizure susceptibility were observed 4 weeks post-SE, potentially due to a mitigated pro-inflammatory response during epileptogenesis.

Materials and Methods

Animal

Adult male C57BL/6J mice aged 8–12 weeks and weighing 22–27 g were provided by the Experimental Animal Center of Anhui Medical University. Animals were housed in a specific pathogen-free environment with a 12-hour light-dark cycle at 21–25°C, and could access food and water freely. This study complied with national legislation regarding the Care and Use of Animals. All protocols were approved by the Ethics Committee of Anhui Medical University.

Experimental Design

Mice were randomly assigned to three groups: (1) control group: mice were injected with saline (10 mL/kg, intraperitoneal (i.p).); (2) SE group: mice were injected with pilocarpine hydrochloride (300 mg/kg, i.p., Topscience, USA); and (3) SE+MCC950 group: SE was induced following MCC950 (20 mg/kg/day, i.p., Glpbio, USA) treatment for 5 days. This study was performed using three cohorts (Figure 1A). First, the levels of biomarkers for M1 and M2 microglia in the hippocampus were investigated 0, 12, 24, and 72 hours post-SE. Seizure susceptibility, video-electroencephalography (VEEG) recording, Morris water maze test, and neuronal damage assay were conducted 4 weeks post-SE. Finally, the pro-inflammatory response in the hippocampus was determined 0, 3, 24, and 72 hours after lipopolysaccharide (LPS) (Escherichia coli 055:B5, 2.5 mg/kg, i.p., Solarbio, China) administration 4 weeks post-SE. Mice injected with saline instead of pilocarpine or LPS were treated as the 0 hour subgroup.

Weight, Consumption of Food and Water

To exclude the possible toxicity of MCC950 at a dose of 20 mg/kg/day (i.p). in mice, the weight and consumption of food and water after drug administration were measured for 4 weeks.

Induction of SE

Mice were pretreated with scopolamine hydrobromide (2 mg/kg, i.p., Glpbio, USA) to prevent peripheral cholinergic effects. After 30 minutes, pilocarpine was injected to induce SE, and reinjection might be needed at an interval of 30 minutes. Behavioral seizures were recorded in five stages as previously described:[23,24] stage 1, chewing, face and

vibrissae twitching, ear rubbing with forepaws; stage 2, head nodding or with unilateral limb clonus; stage 3, bilateral limb clonus or with mild whole-body convulsion; stage 4, lockjaw, tail hypertension with whole-body convulsion; and stage 5, rearing and falling down with whole-body rigidity. SE was defined as a seizure that reached stage ≥ 3 and progressed to repeated or prolonged behavioral seizures. Diazepam (2.5 mg/kg, i.p., Kelun Pharmaceutical Company, China) was administered slowly 120 minutes post-SE to terminate convulsions.

Tissue Preparation

Mice were anesthetized using pentobarbital sodium (40 mg/kg, i.p., YAOPHARMA, China) and perfused transcardially with 25 mL saline. Hippocampal tissue was harvested on ice and immediately stored at −80°C for assays of Western blotting (WB), quantitative real-time PCR (qRT-PCR), and enzyme-linked immunosorbent assay (ELISA). The brains used for immunofluorescence (IF) staining were perfused with 20 mL 4% paraformaldehyde in saline. The brains were dehydrated in 30% sucrose solution for 48 hours and fixed in 4% paraformaldehyde overnight. Next, the brains were covered with OCT compound (Sakura, USA) and cut sequentially into coronal sections (10 μm, Leica, Germany). Sections included the hippocampus were mounted on poly-lysine-coated slides and stored at −80°C.

Western Blot

Hippocampal tissues were homogenized in lysis buffer (150 mM NaCl, 50 mM Tris-HCl 264 (pH 7.4), 1 mM EDTA, 1 mM PMSF, 1% sodium deoxy- 265 cholate, 1% Triton X-100, and 0.1% SDS), centrifuged at 4°C, 12,000 rpm for 10 minutes, and boiled for 15 minutes. The total protein concentration was quantified using a Bicinchoninic Acid Assay (Beyotime, China). Samples (30 μg) were electrophoresed on a 10% sodium dodecyl sulfate-polyacrylamide gel at 55 V for 60 minutes, and then at 110 V for 60 minutes. Proteins were transferred onto PVDF membranes (Immobilon-P, Millipore, USA) at 20 mA for 225 minutes and blocked with 5% non-fat milk for 1.5 hours at room temperature (RT). After 15 minutes wash in triple-distilled water, membranes were incubated at 4°C overnight with primary antibodies: rabbit anti-NLRP3 (1:1,000, Proteintech, China), mouse anti-CD206 (1:2,000, Proteintech, China), rabbit anti-CD16/32 (1:1,000, Abcam, USA), and mouse anti-β-actin (1:5,000, Proteintech, China). After four washes with PBST, the membranes were incubated with the corresponding secondary antibodies, goat anti-rabbit IgG (1:10,000, ZSGB-BIO, China) and goat anti-mouse IgG (1:10,000, ZSGB-BIO, China), for 2 hours at RT. The membranes were washed with four PBST solutions and developed using an enhanced chemiluminescence kit (Thermo Scientific, USA). Images were captured using a Tanon developer (Tanon Fine-do X6; China). Image J software (version 1.53t, USA) was used to analyze the protein bands.

Immunofluorescence Staining

The sections were permeabilized with 0.3% Triton X-100 (Servicebio, China) for 40 minutes at RT. After three PBS washes, sections were blocked with 5% Albumin Bovine V (Biosharp, China) at RT for 1 hour and then incubated with primary antibodies at 4°C overnight: rat anti-NLRP3 (1:100, Novusbio, USA), goat anti-TSPO (1:100, Novusbio, USA), rabbit anti-CD16/32 (1:100, Novusbio, USA), rabbit anti-CD206 (1:100, Novusbio, USA), rabbit anti-NueN (1:400, CST, USA), rabbit anti-Iba-1 (1:400; Wako, Japan), and mouse anti-GFAP (1:400, CST, USA). Sections were washed five times with PBS and incubated with secondary antibodies at RT in the dark for 2 hours: goat anti-rat FITC (1:100, ZSGB-BIO, China), rabbit anti-goat Alexa Fluor® 488 (1:400, ZSGB-BIO, China), goat anti-rabbit Alexa Fluor® 594 (1:400, ZSGB-BIO, China), and goat anti-mouse Alexa Fluor® 488 (1:400, Abcam, USA). After five PBS washes, the sections were stained with DAPI (Servicebio, China) for 5 minutes at RT, washed with DAPI, and covered with antifade mounting medium (Servicebio, China). Images were acquired under the same exposure conditions by using a fluorescence microscope (Leica, Germany). Fluorescence-positive cells and fluorescence intensity were measured using the Image J software (version 1.53t, USA).

Quantitative Real-time PCR

Total RNA was extracted using TRIzol reagent (Invitrogen, USA) following the manufacturer's protocol. One microgram of total RNA was reverse-transcribed using a Reverse Transcription System (Bio-Rad, USA), and cDNA was stored at −20°C. Amplification was conducted using the StepOnePlus™ real-time PCR system (ABI, USA). Reverse transcription was performed in a final volume of 20 μL containing 3 μL cDNA, 0.4 μL forward and reverse primer (10 μM), 10 μL

2×SYBR Green qPCR Master Mix, and 6.2 μL RNase free water. The cycling conditions were 40 cycles, including denaturation at 95°C for 30 seconds, primer annealing for 30 seconds at 60°C, and primer extension at 95°C for 15 seconds. β-actin mRNA was used as an internal reference gene. Relative gene expression was analyzed using $2^{-\Delta\Delta Ct}$ method. Primer sequences were as follows: NLRP3, forward primer: 5′-CCAGGGCTCTGTTCATTG-3′, reverse primer: 5′-CCTTGGCTTTCACTTCG-3′; Caspase-1, forward primer: 5′-AGGAGGGAATATGTGGG-3′, reverse primer: 5′-AACCTTGGGCTTGTCTT-3′; CD16, forward primer: 5′-CCAGGTCCAATCCAGCTACA-3′, reverse primer: 5′-TTGTTCCTCCAGCTATGGCA-3′; CD206, forward primer: 5′-AGTGGCTTTGGTTGAACGAC-3′, reverse primer: 5′-CCAAAGGCCCGAAGATGAAG-3′; iNOS, forward primer: 5′-ACCATGAGGCTGAAATCCCA-3′, reverse primer: 5′-ATCCACAACTCGCTCCAAGA-3′; Arg-1, forward primer: 5′-CACAGACAGCAAGGTGTACG-3′, reverse primer: 5′-TCTGTCCGTTCCATTTCCCA-3′; β-actin, forward primer: 5′-AGTGTGACGTTGACATCCGT-3′, reverse primer: 5′-TGCTAGGAGCCAGAGCAGTA-3′.

Enzyme-Linked Immunosorbent Assay

The concentrations of IL-1β, IL-18, and TGF-β in the hippocampus were determined using an ELISA kit (Ruixin Biotech, China), according to the manufacturer's instructions.

Morris Water Maze Test

The Morris water maze (MWM) test (Sansbio, China) consisted of a black circular pool (120 cm diameter and 40 cm height). The pool is divided into four quadrants. In the target quadrant, a circular platform with 7.5 cm was submerged 1 cm below water. White pigment was mixed with water to obtain an opaque appearance. Four markers of different colors and shapes were posted on the walls of the four quadrants. In the place navigation test, mice were trained four times with an interval of 20 minutes for 4 days. Each trial allowed mice to swim freely for 60 seconds. Mice entered the water at four inlet points in each quadrant, facing the wall with their heads. Escape latency (time spent from the start point to the platform) was recorded. Mice were guided to the platform and stayed there for 15 seconds; if they were unable to find the platform within 60 seconds, the escape latency was recorded as 60 seconds. The platform was removed on the fifth day of the spatial probe test. Mice were released from the inlet point opposite to the target quadrant and allowed to swim for 90 seconds. After each training session, the mice were wiped dry and kept warm before returning to their cage.

6-Hz Psychomotor Seizure Test

The 6-Hz test was conducted as described by Socala et al.[25] Before stimulation, 50 μL of 0.5% tetracaine hydrochloride ophthalmic solution was bilaterally applied to the corneas. The corneal electrodes were coated with a thin layer of electrode gel. A constant-current device (Ugo Basile ECT Unit, Italy) was used to deliver a current at 0.2 ms pulse-width, 3 s duration, and 6 pulses/s frequency. CC50 (intensity of current for the induction of seizures in 50% of animals) was measured as a parameter for seizure susceptibility. Each mouse was tested only once. A preliminary experiment was conducted to identify 20 mA as the CC50 for wild-type C57BL/6 mice. Current intensity was established according to an "up-and-down" method.[26] A current of 20 mA was administered to the first mouse in each group, followed by an increase or decrease at 0.06-log interval. The mice were restrained during stimulation and then released into transparent cages for behavioral observations. 6-Hz induced psychomotor seizures were characterized by stun, rearing, forelimb clonus, twitching of vibrissae, and an elevated tail. Mice were scored as protected from seizure if they did not show behavioral seizure or resumed normal exploratory behavior within 10 seconds. Seizure threshold (CC50) was determined as described by Kimball et al.[26]

Picrotoxin Induced Seizure

Mice were injected with picrotoxin (2.0 mg/kg, i.p., Topscience, China), followed by recording for 30 minutes at 5 minute intervals. Behavioral seizures were scored as previously described.[27] Briefly, stage 1, immobility; stage 2, forelimb or tail stretch; stage 3, recurrent circling or scratching; stage 4, rearing and falling; stage 5, repetitive behavior of stages 2–4; stage 6, rigidity with convulsions; and stage 7, death.

Electrode Implantation and VEEG Recording

Mice were anesthetized with isoflurane (3.5% induction, 1.5% maintenance) and fixed on a stereotaxic apparatus (RWD Life Science, China). A rostrocaudal incision was made in the skull skin and disinfected with 1% iodophor. Medical hydrogen peroxide was used to remove the soft tissue and expose the bregma and posterior fontanelle. After adjusting bregma and posterior fontanelle to a horizontal level, holes were drilled on the skull over the hippocampus following the Mouse Brain in Stereotaxic Coordinates (2nd edition, Paxinos and Franklin):[28] 2.0 mm posterior to bregma, ± 2.25 mm lateral, 0.25 mm ventral to the skull. Bilateral EEG recording electrodes (Nanjing Greathink Medical Technology, Nanjing, China) were implanted epidurally. Two electrodes positioned in the skull over the frontal lobe and the cerebellum was used as the ground and reference, respectively. Two copper wires were inserted into the cervical muscles to record electromyography. The electrodes were fixed with screws and dental acrylic cement. Mice were injected with ampicillin (100 mg/kg, i.p., Kelun Pharmaceutical Company, China) for 3 days to prevent infection. After 5 days of recovery, the mice were subjected to VEEG recording using a multi-channel physiological signal recording system (Nanjing Greathink Medical Technology, China). Before recording, the mice were allowed to habituate to the test cage for 1 hour. Each mouse was recorded daily for 12 h (6:00–18:00) during the latency period (the time from SE induction to the first spontaneous recurrent seizures (SRSs)) and epileptogenesis (fourth week post-SE). EEG was down-sampled at 500 Hz and band-pass filtered from 5 to 80 Hz with a 50-Hz notch filter. Epileptiform spikes were detected and counted using SIRENIA® SEIZURE (Pinnacle Technology, USA). A spike was defined as a sharp deflection with an amplitude at least three times higher than the background for a duration of 20–100 ms.[29] For SRSs detection, epileptic seizures were identified by a cluster of spikes that persisted for more than 10 seconds. All electrographic seizures were confirmed using a video.

Statistical Analysis

The distribution of all data was evaluated by calculating the kurtosis and skewness. Data are presented as mean ± SD or median (interquartile range [IQR]) for variables with normal or skewed distributions, respectively. Student's *t*-test, Mann–Whitney *U*-test, and one-way analysis of variance (ANOVA) followed by least significant difference (LSD) post hoc tests were used to analyze differences among groups. Differences in escape latency during 4 training days in the Morris water maze among groups were analyzed using a repeated measures two-way ANOVA. Kaplan-Meier analysis was used to determine the latency to SRSs. All graphs were performed using GraphPad Prism (version 8.4.2, USA). In immunofluorescence assay, fluorescent positive cells and mean fluorescence intensity were measured by Image J (version 1.54f, USA). Image J was also used in Western blot to analyze the value of each sample band normalized with corresponding internal reference. Images were managed with Adobe Photoshop CS6 (Adobe, USA). Statistical analysis was performed using SPSS software (version 22.0; IBM Inc., USA). $P < 0.05$ was considered as statistically significant.

Results

Influence of MCC950 on Survival

After monitoring for 4 weeks, no significant differences were observed in weight, food, or water consumption between mice treated with MCC950 for 5 days at 20 mg/kg (i.p). and those treated with saline (Figure 1B–D). After SE induction, the results showed that weight and food and water consumption in the SE+MCC950 group were significantly higher than those in the SE group on both the fourth or fifth day (Figure 1E–G). No difference was noted in survival between the two groups during epileptogenesis (2 weeks post-SE, Figure 1E–G). These results suggest that MCC950 administration has no detrimental effects on mice and may assist with recovery from SE.

Hippocampal Microglia Tend to Polarize into M1 Phenotype in SE Mice

Within the first 72 hours post-SE, WB, PCR, and IF revealed that CD16/32 expression was markedly increased compared to that at 0 hours, reaching its peak at 24 hours (Figure 2A–E). A similar tendency was observed for IL-1β expression, which is secreted by M1 microglia (Figure 2F). Simultaneously, a significant decrease in CD206 and TGF-β expression was detected within 72 hours post-SE (Figure 2A, B and G–J). These results suggest that microglia in the hippocampus of SE mice are prone to differentiate into the M1 phenotype.

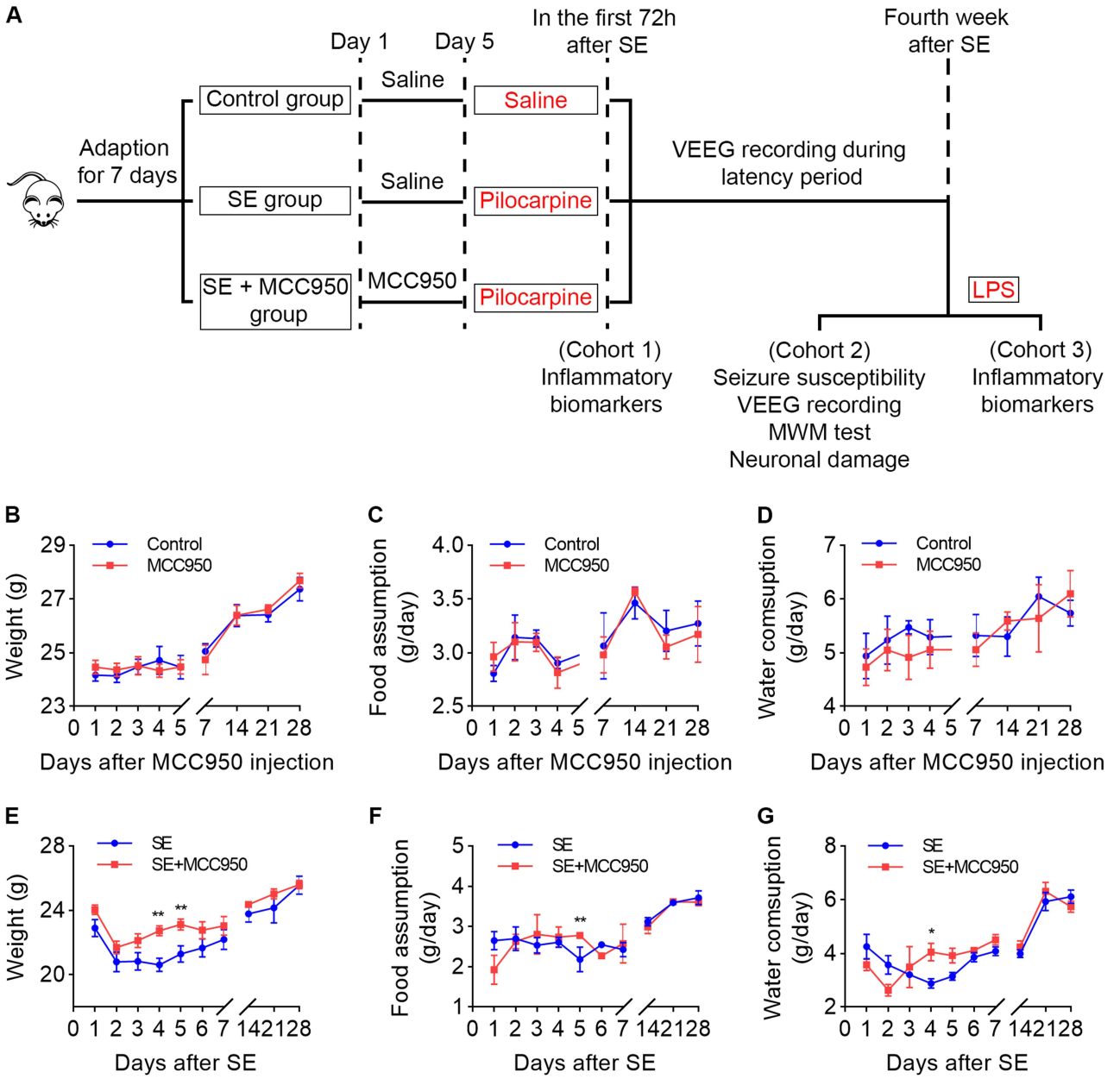

Figure 1 (**A**) Diagram of experimental procedure; (**B–D**) Weight, food, and water consumption in mice without SE; (**E–G**) Weight, food, and water consumption in epileptic mice.

Notes: * $P < 0.05$, ** $P < 0.01$ by Student's *t*-test (**B–G**). Values are means ± SD (**B–G**).

NLRP3 Inflammasome Inhibition Modulates Microglial Polarization Post-SE

The expression of hippocampal NLRP3 in SE mice pretreated with MCC950 was significantly suppressed compared to that in the SE group within the first 72 hours post-SE (Figures 2A and 3A–C). Similarly, the mRNA levels of NLRP3 and Caspase-1 were markedly decreased in the SE+MCC950 group compared to the SE group (Figure 3D and E). Additionally, IL-1β and IL-18 levels were obviously increased in SE mice without MCC950 treatment (Figures 2F and 3G). These results indicated that the hippocampal NLRP3 inflammasome is activated in SE mice and can be effectively inhibited by MCC950 for at least 72 hours post-SE.

Next, we detected the expression of M1 and M2 microglia biomarkers in the hippocampus. The translocator protein (TSPO) was highly expressed within 72 hours post-SE in both groups, however, a significantly reduced level of TSPO was observed in

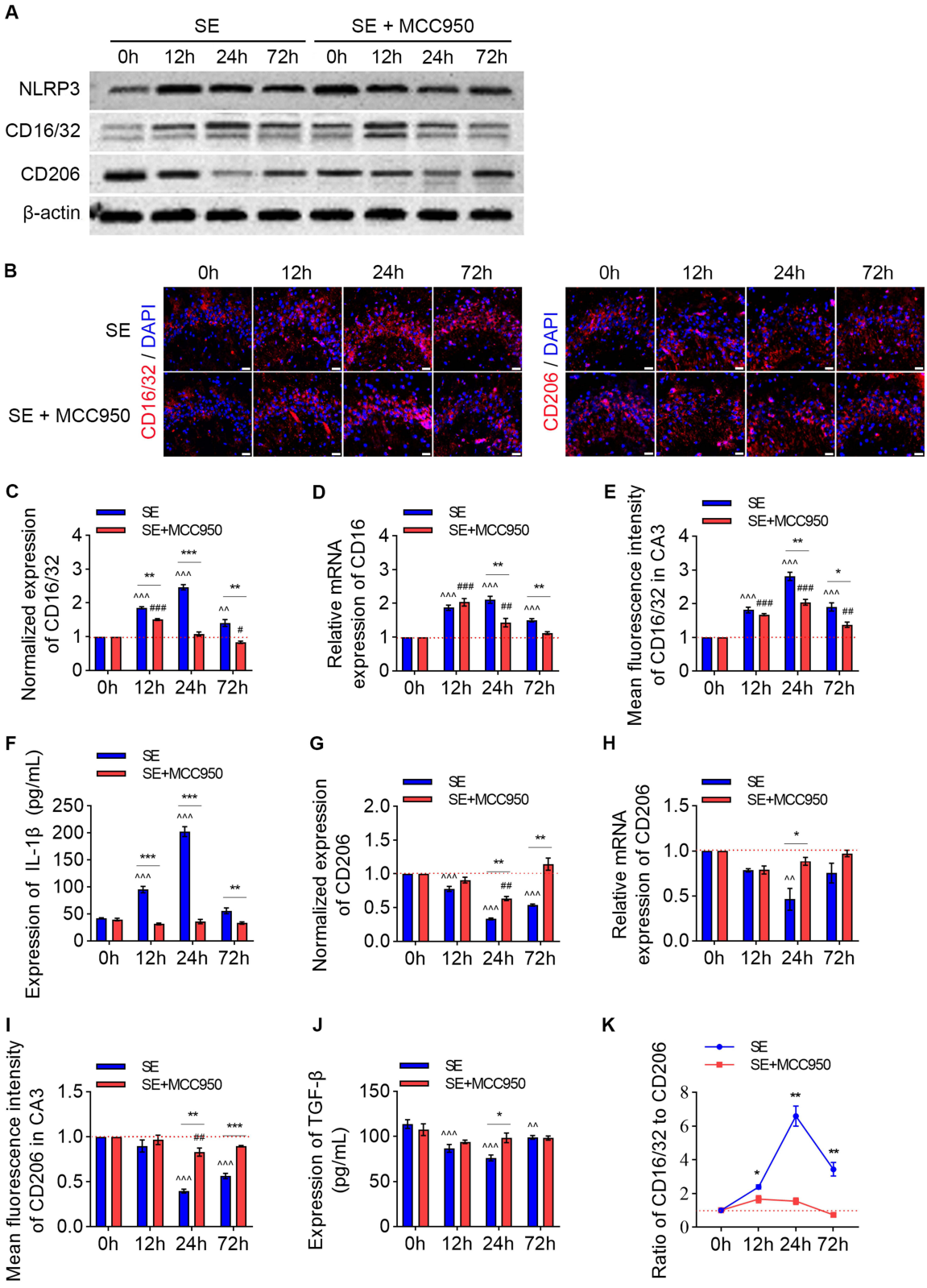

Figure 2 Determination of biomarkers for microglia after SE. (**A**) WB determined protein expression of NLRP3, CD16/32, and CD206; (**B**) Expression of CD16/32 and CD206 in the hippocampus determined by IF; (**C**) Normalized expression of CD16/32 based on WB; (**D**) The mRNA expression of CD16 determined by RT-qPCR; (**E**) Mean fluorescence intensity of CD16/32 in CA3 based on IF; (**F**) Expression of IL-1β determined by ELISA; (**G**) Normalized expression of CD206 based on WB; (**H**) The mRNA expression of CD206 determined by RT-qPCR; (**I**) Mean fluorescence intensity of CD206 in CA3 based on IF; (**J**) Expression of TGF-β determined by ELISA; (**K**) Relative ratio of CD16/32 to CD206 based on WB.
Notes: * $P < 0.05$, ** $P < 0.01$, *** $P < 0.001$; ^^ $P < 0.01$, ^^^ $P < 0.001$; # $P < 0.05$, ## $P < 0.01$, ### $P < 0.001$ by Student's *t*-test between two groups at each timepoint (**C**–**K**), One-way ANOVA with LSD test among different timepoints within each group (**C**–**J**). Values are means ± SD (**C**–**K**). Scale bar: 25 μm (**B**).

the SE+MCC950 group compared to the SE group (Figure 3A and F), suggesting an attenuated microglial activation in SE mice pretreated with MCC950. CD16/32 expression was obviously increased in the SE group at 24 and 72 hours post-SE compared to the SE+MCC950 group (Figure 2A–E), whereas CD206 expression exhibited an adverse trend, being dramatically decreased in the SE group at 24 hours (Figure 2A, B and G–I). Consequently, the relative ratio of CD16/32 to CD206, based on WB analysis, was significantly higher in the SE group (Figure 2K). Additionally, IL-1β levels were significantly elevated, while TGF-β levels were significantly reduced in the SE group compared to the SE+MCC950 group (Figure 2F and J), indicating a weaker pro-inflammatory response in SE mice pretreated with MCC950. These findings suggest that NLRP3 inflammasome inhibition diminishes microglial polarization towards the M1 phenotype in the hippocampus post-SE.

NLRP3 Inflammasome Inhibition Post-SE Alleviates Seizure Susceptibility During Epileptogenesis

First, we measured the 6-Hz seizure threshold 4 weeks post-SE. Compared to the SE group (13.26 ± 1.55 mA), a drastically increased seizure threshold was found in the control (24.82 ± 0.74 mA) and SE+MCC950 groups (23.81

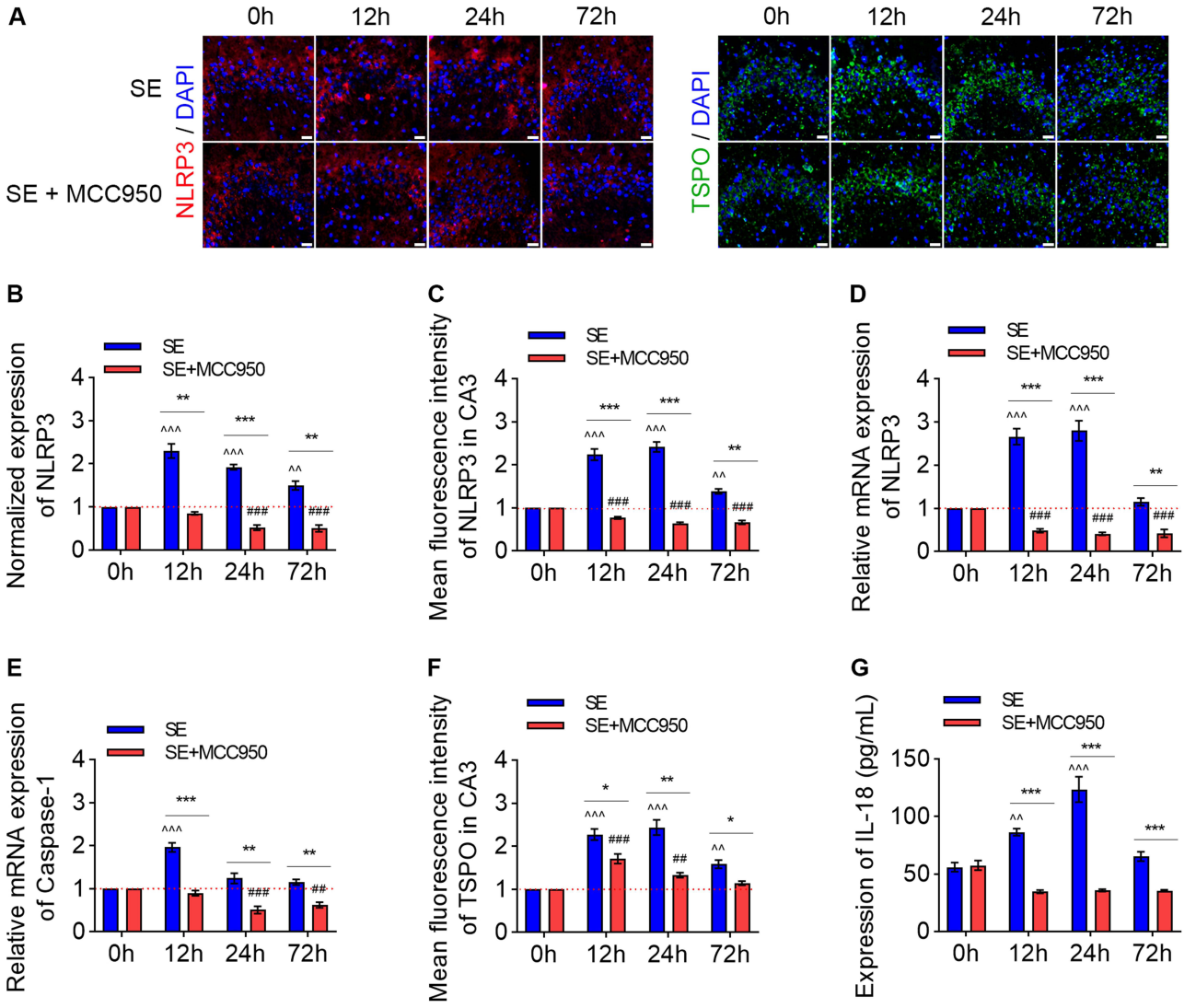

Figure 3 Determination of NLRP3 inflammasome after SE. (**A**) Expression of NLRP3 and TSPO in the hippocampus determined by IF; (**B**) Normalized expression of NLRP3 based on WB; (**C**) Mean fluorescence intensity of NLRP3 in CA3 based on IF; (**D**) The mRNA expression of NLRP3 determined by RT-qPCR; (**E**) The mRNA expression of Caspase-1 determined by RT-qPCR; (**F**) Mean fluorescence intensity of TSPO in CA3 based on IF; (**G**) Expression of IL-18 determined by ELISA.

Notes: * $P < 0.05$, ** $P < 0.01$, *** $P < 0.001$; ^^ $P < 0.01$, ^^^ $P < 0.001$; $^{\#\#}$ $P < 0.01$, $^{\#\#\#}$ $P < 0.001$ by Student's *t*-test between two groups at each timepoint (**B**–**G**), One-way ANOVA with LSD test among different timepoints within each group (**B**–**G**). Values are means ± SD (**B**–**G**). Scale bar: 25 μm (**A**).

± 3.68 mA) (Figure 4A). Next, seizure scores were evaluated following picrotoxin administration, a non-competitive inhibitor of the GABAα receptor. Thirty minutes after picrotoxin injection, the seizure score significantly increased in the SE group compared to the other groups (Figure 4B). No significant differences in seizure threshold or seizure score were observed between the control and SE+MCC950 groups (Figure 4A and B).

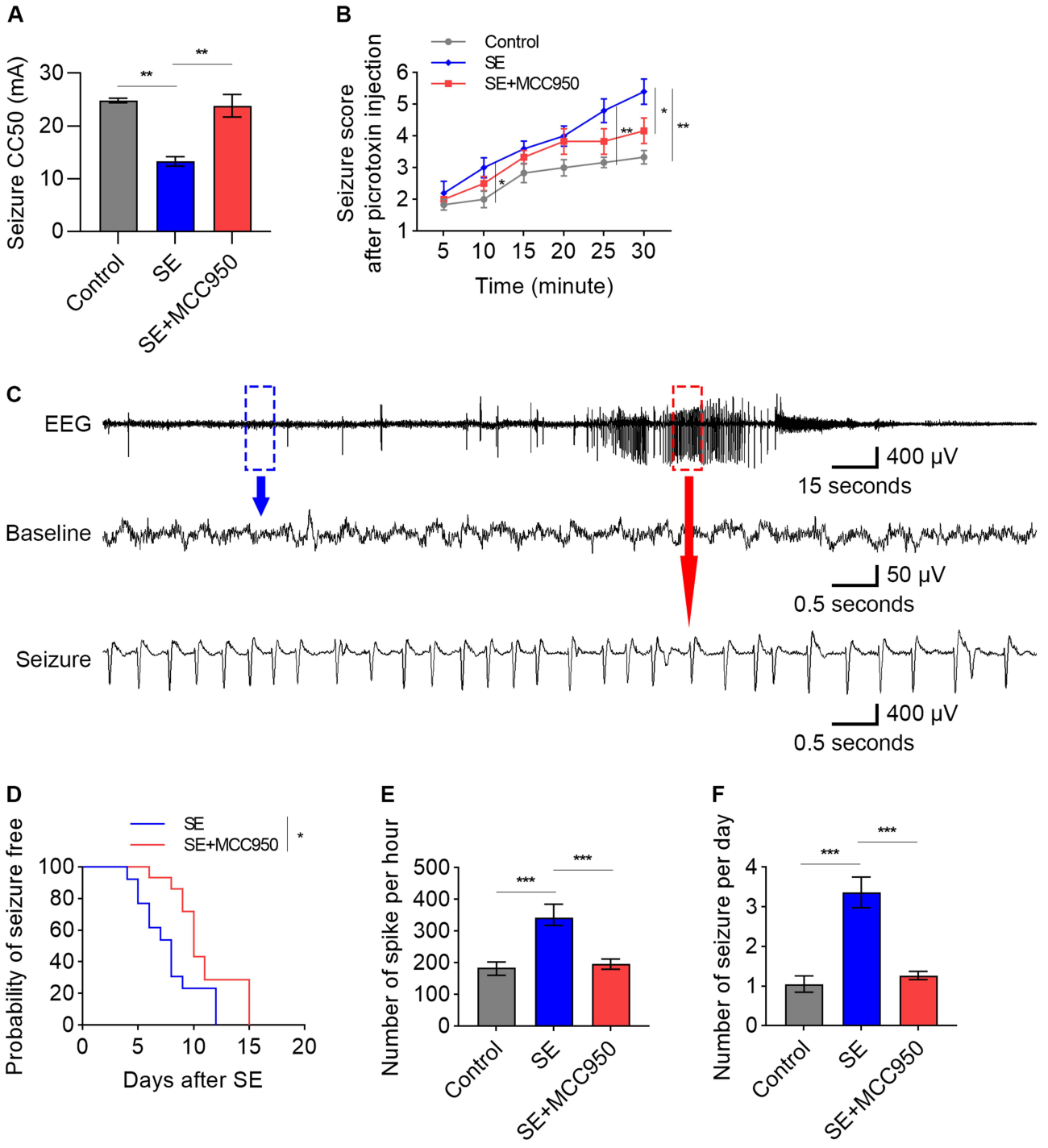

Figure 4 Seizure susceptibility measured at 4 weeks after SE. (**A**) 6-Hz seizure threshold; (**B**) Seizure score after picrotoxin treatment; (**C**) Representative diagram of EEG, baseline, and seizure; (**D**) Latency to spontaneous recurrent seizures (SRSs); (**E**) Electroencephalographic discharges per hour; (**F**) Frequency of spontaneous recurrent seizures per day.

Notes: * $P < 0.05$, ** $P < 0.01$, *** $P < 0.001$ by One-way ANOVA with LSD test (**A, B, E**, and **F**), Kaplan-Meier analysis with Log Rank (Mantel-Cox) test (**D**). Values are means ± SD (**A, B, E**, and **F**).

Finally, we analyzed the seizure activity during epileptogenesis using VEEG recordings (Figure 4C). The results displayed that the latency to SRSs was obviously prolonged in the SE+MCC950 group (9.91 ± 0.67 days) compared to the SE group (7.09 ± 0.68 days) (Figure 4D). At 4 weeks post-SE, epileptiform discharge was significantly enhanced in the SE group (349.80 ± 38.31 spikes/h) compared to the control (182.40 ± 23.46 spikes/h) and SE+MCC950 groups (196.20 ± 16.99 spikes/h) (Figure 4E). Similarly, the frequency of SRSs was markedly increased in the SE group (3.37 ± 0.94 SRSs/day) compared to the control (1.11 ± 0.20 SRSs/day) and SE+MCC950 groups (1.27 ± 0.26 SRSs/day) (Figure 4F). These results suggest that neuronal networks in epileptic brains exhibit an enhanced susceptibility to seizures. Hippocampal NLRP3 inflammasome inhibition post-SE ameliorates the hyperexcitability observed in epileptic brains.

NLRP3 Inflammasome Inhibition Post-SE Improves Neuronal Loss and Cognitive Dysfunction in SE Mice

Compared to the control and SE+MCC950 groups, SE mice exhibited significantly stronger neuronal loss in CA3 four weeks post-SE (Figure 5A and C). Furthermore, the number of Iba-1$^+$ and GFAP$^+$ cells in the hippocampus was markedly higher in the SE group compared to the other groups (Figure 5A, D and E). The MWM test was employed to assess cognitive dysfunction (Figure 5B). During the place navigation test, escape latency for all three groups gradually decreased over the 4 training days, but no significant differences were observed among them (Figure 5G). In the spatial probe test, mice in the SE group took the longest time to arrive the platform compared to the other groups (Figure 5F). Additionally, the SE group exhibited significantly fewer platform crossings and time spent in the target quadrant within 60 seconds compared to the other groups (Figure 5H and I). Collectively, these results indicate that NLRP3 inflammasome inhibition post-SE protects against neuronal loss, gliosis, and improves cognitive dysfunction in the development of epilepsy.

NLRP3 Inflammasome Inhibition Post-SE Protects the Brain Against LPS-Induced Inflammatory Response

To verify the increased pro-inflammatory susceptibility in the epileptic brain during epileptogenesis, we determined the expression of M1 and M2 microglial biomarkers in the hippocampus following LPS administration 4 weeks post-SE. To avoid the confounding effects of an intense inflammatory response on the baseline pro-inflammatory status, we first determined a mild pro-inflammatory stimulation induced by LPS. As shown in Figure 6A, the mRNA levels of CD16 and CD32 were significantly elevated after a low dose of LPS (2.5 mg/kg); thus, this dose was selected for further experiments.

Compared to 0 hours, the expression of CD16/32 was significantly elevated in all groups within 72 hours and peaked at 24 hours after LPS treatment (Figure 6B and C). A similar trend was observed in the mRNA levels of CD16 and iNOS, as well as IL-1β (Figure 6D–F), which were highly expressed at 24 hours in the SE group compared to the other groups. Conversely, CD206 expression significantly decreased 24 hours after LPS administration in the SE group compared to the other groups (Figure 6B and G). This trend was also observed in the mRNA levels of CD206 and Arg-1, as well as in TGF-β levels (Figure 6H–J). These results suggest that the epileptic brain exhibits an enhanced pro-inflammatory susceptibility, which can be attenuated by the inhibition of NLRP3 inflammasome post-SE.

Taken together, NLRP3 inflammasome inhibition after pilocarpine-induced status epilepticus restrains epileptogenesis in epileptic mice, which may be attributed to improved hippocampal neuronal loss and decreased chronic pro-inflammation susceptibility.

Discussion

In this study, we have observed that pretreatment with MCC950 in SE mice enhanced neuronal protection, reduced seizure susceptibility, and improved cognitive function during epileptogenesis. These beneficial effects are likely attributable to the attenuated pro-inflammatory susceptibility resulting from inhibition of the NLRP3 inflammasome post-SE.

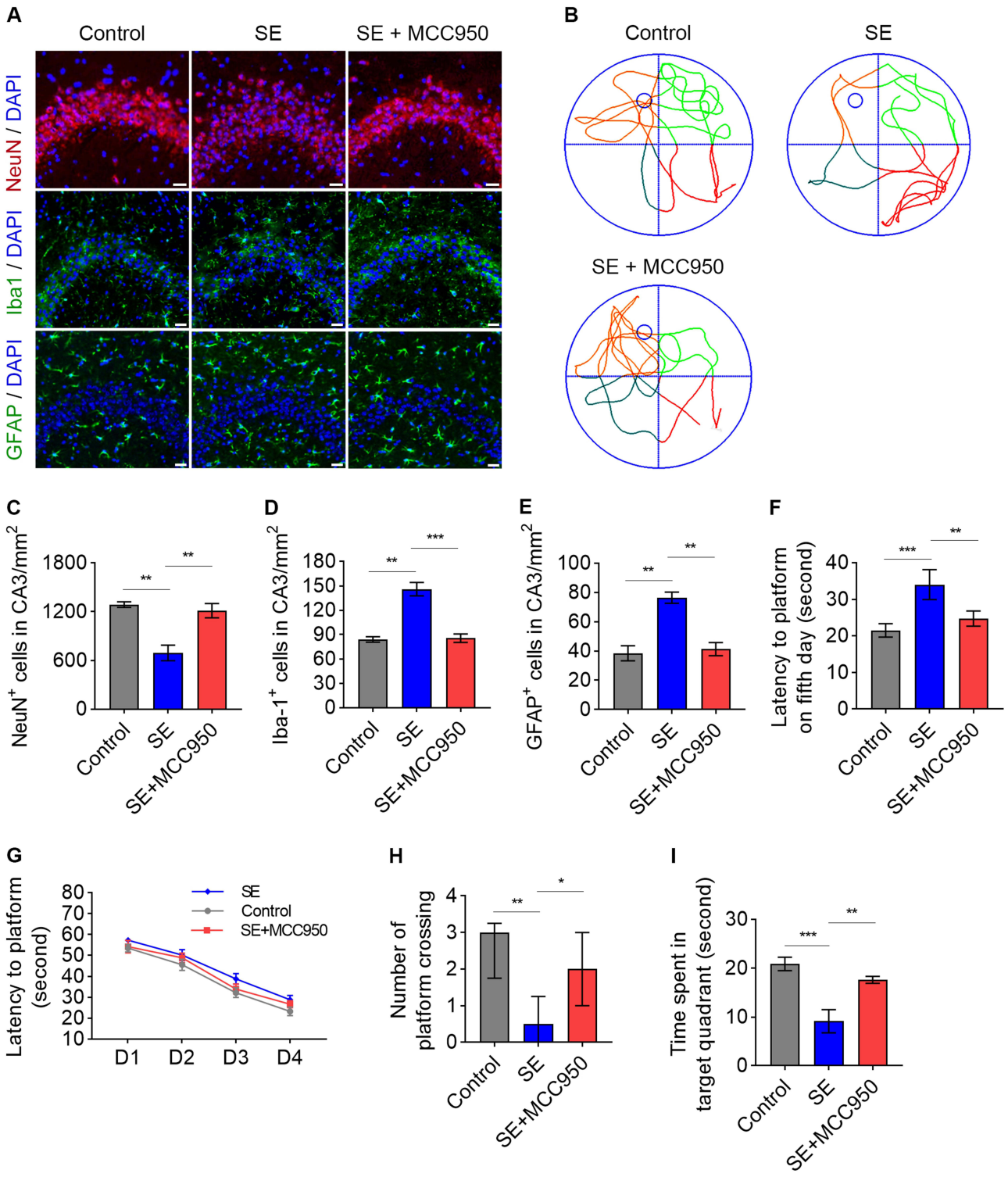

Figure 5 Neuronal damage assay and cognition test. (**A**) Expression of $NeuN^+$, Iba-1^+, and $GFAP^+$ cells in hippocampus determined by IF; (**B**) Representative diagram of Morris water maze test; (**C**) Number of $NeuN^+$ cells in CA3 based on IF; (**D**) Number of Iba-1^+ cells in CA3 based on IF; (**E**) Number of $GFAP^+$ cells in CA3 based on IF; (**F**) Escape latency on the fifth day; (**G**) Escape latency over 4 training days; (**H**) Number of platform crossings; (**I**) Time spent in target quadrant.

Notes: $^*P < 0.05$, $^{**}P < 0.01$, $^{***}P < 0.001$ by One-way ANOVA with LSD test (**C**–**F**, and **I**), repeated measures two-way ANOVA among three groups during 4 training days (**G**), Mann–Whitney *U*-test (**H**). Values are means ± SD (**C**–**G**, and **I**) and medians (IQR) (**H**). Scale bar: 25 μm (**A**).

https://doi.org/10.2147/JIR.S469451 DovePress

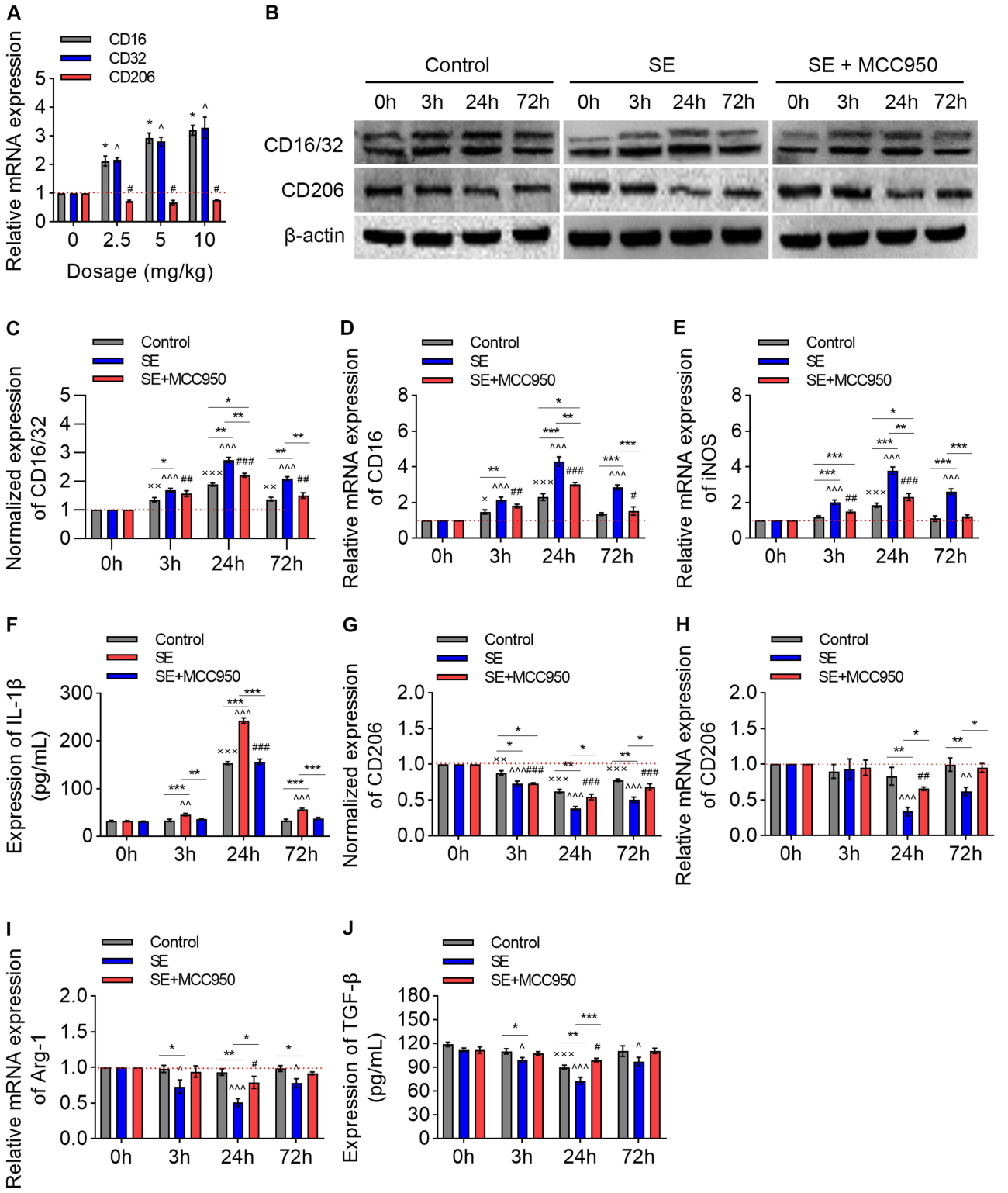

Figure 6 Determination of biomarkers for microglia after LSP treatment. (**A**) The mRNA expression of CD16, CD32, and CD206 determined by RT-qPCR at different doses of LPS; (**B**) WB determined protein expression for control, SE, and SE+MCC950 groups; (**C**) Normalized expression of CD16/32 based on WB; (**D**) The mRNA expression of CD16 determined by RT-qPCR; (**E**) The mRNA expression of iNOS determined by RT-qPCR; (**F**) Expression of IL-1β determined by ELISA; (**G**) Normalized expression of CD206 based on WB; (**H**) The mRNA expression of CD206 determined by RT-qPCR; (**I**) The mRNA expression of Arg-1 determined by RT-qPCR; (**J**) Expression of TGF-β determined by ELISA.

Notes: * $P < 0.05$, ** $P < 0.01$, *** $P < 0.001$; ^ $P < 0.05$, ^^ $P < 0.01$, ^^^ $P < 0.001$; # $P < 0.05$, ## $P < 0.01$, ### $P < 0.001$; × $P < 0.05$, ×× $P < 0.01$, ××× $P < 0.001$ by One-way ANOVA with LSD test among different dosages within each group (**A**), One-way ANOVA with LSD test among three groups at each timepoint (**C**–**J**) and among different timepoints within each group (**C**–**J**). Values are means ± SD (**C**–**J**).

Numerous studies have highlighted the role of inflammatory pathways activation on epilepsy.[8,9,12,30,31] Microglia, as resident immune cells in the central nervous system, are involved in phagocytosis, cell proliferation, and cytokine production.[32] Epilepsy is well-documented to elicit microglial activation, which can exacerbate brain inflammation.[9] The serum levels of IL-6 are significantly reduced in patients with well-controlled generalized epilepsy during valproate therapy.[33] Interleukin-10, a reparative cytokine, regulates the basal phenotype of microglia in the hippocampus with neuronal damage,[9] and inhibits IL-1β production in epileptic mice,[16] Our findings revealed that M1 microglial biomarkers, including CD16/32, iNOS, and IL-1β, were highly expressed post-SE. Conversely, there was a significant reduction in the expression of CD206, Arg-1, and TGF-β, which are used as biomarkers for M2 microglia. These results suggest that a preferential proliferation of microglia towards the M1 phenotype post-SE.

Microglia are activated within epileptic foci and release pro-inflammatory cytokines.[34,35] It has been confirmed that inflammatory cytokines, such as IL-1β, accelerate neuronal loss and enhance neuronal excitability.[21,36] The upregulation of M1 microglia post-SE may contribute to more frequent seizures during epileptogenesis.[11] Inflammation strengthens neuronal excitability and reduces the seizure threshold in a vulnerable epileptic brain,[37] supporting the notion that a pro-inflammatory status is a promoter of epileptogenesis. Therefore, it is beneficial to explore potential strategies to balance microglial polarization in antiepileptogenesis.

The NLRP3 inflammasome is mainly expressed in microglia,[18] and its activation has been implicated in the polarization of activated microglia towards a pro-inflammatory phenotype.[16,20,21,36,38] Suppression of the NLRP3 inflammasome inhibits neuroinflammation mediated by microglia.[38] Interleukin-10 potently suppressed IL-1β production in the microglia of epileptic mice by inhibiting NLRP3 inflammasome activity.[16] Additionally, NLRP3 inflammasome inhibition alleviates LPS-induced inflammatory response in BV2 microglial cells.[22] The NLRP3 inflammasome can be activated by elevated extracellular ATP, reactive oxygen species production, increased intracellular Ca^{2+}, and hypoxia,[39] all of which are implicated in epileptogenesis.[40,41] Our study demonstrated that the NLRP3 inflammasome inhibition post-SE significantly decreased pro-inflammatory cytokines levels, which may be attributed to attenuated M1 microglial proliferation. During the SRSs period, SE mice with NLRP3 inflammasome inhibition exhibited improvements in neuronal damage, seizure susceptibility, and cognitive function. Therefore, the dampened polarization of M1 microglia resulted from NLRP3 inflammasome inhibition post-SE plays a potential role in mitigating epileptogenesis.

In this study, LPS (2.5 mg/kg, i.p). was used to stimulate inflammation in the epileptic brain 4 weeks post-SE, revealing that biomarkers for activated M1 microglia, such as CD16/32, IL-1β, and iNOS, significantly elevated in SE mice compared to the control and SE+MCC950 groups. Inflammation characterized by microglia activation and IL-1β overexpression was evident in the hippocampus of patients with temporal lobe epilepsy.[35] In animal experiments, a sustained elevation of IL-1β mRNA levels, approximately two-fold higher, has been observed 3 weeks post-SE.[11] These evidence demonstrate that the epileptic brain suffers from chronic pro-inflammatory susceptibility during epileptogenesis, potentially resulting from a less permissive pathological environment surrounding neurons, including microglial activation.[42] In our study, SE mice pretreated with MCC950 showed obviously reduced levels of M1 microglial biomarkers following LPS administration, suggesting that the inhibition of NLRP3 inflammasome post-SE suppress microglial activation and thereby attenuate pro-inflammatory susceptibility during epileptogenesis.

Our investigation underscores the critical role of persistent inflammatory status during epileptogenesis. Inactivating NLRP3 inflammasome post-SE decreased seizure susceptibility and exerted neuroprotective effects in the epileptic brain, suggesting that the modulation of NLRP3 inflammasome could be a promising therapeutic target for antiepileptogenesis. However, several limitations should be acknowledged. Firstly, NLRP3 inflammasome inhibition suppressed microglial activation, we failed to determine whether the activation of microglia was primarily induced by SE or NLRP3 inflammasome activation. There is currently no evidence to support that NLRP3 inflammasome stimulates microglial activation. Secondly, we did not confirm whether microglia with increased pro-inflammatory susceptibility during epileptogenesis were the same population that was activated during the acute period post-SE. Consequently, the relationship between the NLRP3 inflammasome and microglia, as well as the population of activated microglia that progresses into a chronic inflammatory status during epilepsy development, needs to be investigated.

Conclusion

In summary, hippocampal microglia in SE mice demonstrated a propensity towards differentiation into the M1 phenotype. Inhibition of NLRP3 inflammasome post-SE ameliorates neuronal loss, seizure susceptibility, and cognitive function during epileptogenesis. These effects are likely attributed to the attenuated polarization of M1 microglia during the acute period following SE, as well as the mitigated chronic pro-inflammatory response in the epileptic brain. Our findings may provide novel insights into the pathogenesis of epileptogenesis, underscoring the importance of early anti-inflammation post-SE in attenuating epileptogenesis, although further mechanisms remain to be explored.

Data Sharing Statement

The datasets used or analyzed during the current study are available from the corresponding author upon reasonable request.

Ethics Approval

This study complied with national legislation on the Care and Use of Animals. All protocols were approved by the Ethics Committee of Anhui Medical University.

Acknowledgment

We thank the Center for Scientific Research of Anhui Medical University for providing instructions for immunohistochemical analysis.

Author Contributions

All authors made a significant contribution to the work reported, whether that is in the conception, study design, execution, acquisition of data, analysis and interpretation, or in all these areas; took part in drafting, revising or critically reviewing the article; gave final approval of the version to be published; have agreed on the journal to which the article has been submitted; and agree to be accountable for all aspects of the work.

Funding

This study was supported by grants from the National Natural Science Foundation of China (No. 82071460, Yu Wang).

Disclosure

The authors declare that they have no known competing financial interests or personal relationships that could influence the work reported in this study.

References

1. Thijs RD, Surges R, TJ O, Sander JW. Epilepsy in adults. *Lancet*. 2019;393(10172):689–701. doi:10.1016/S0140-6736(18)32596-0
2. Manford M. Recent advances in epilepsy. *J Neurol*. 2017;264(8):1811–1824. doi:10.1007/s00415-017-8394-2
3. Kanner AM, Bicchi MM. Antiseizure Medications for Adults With Epilepsy: a Review. *JAMA*. 2022;327(13):1269–1281. doi:10.1001/jama.2022.3880
4. Perucca P, Scheffer IE, Kiley M. The management of epilepsy in children and adults. *Med J Aust*. 2018;208(5):226–233. doi:10.5694/mja17.00951
5. Poniatowski ŁA, Cudna A, Kurczych K, Bronisz E, Kurkowska-Jastrzębska I. Kinetics of serum brain-derived neurotrophic factor (BDNF) concentration levels in epileptic patients after generalized tonic-clonic seizures. *Epilepsy Res*. 2021;173:106612. doi:10.1016/j.eplepsyres.2021.106612
6. Chugh D, Ali I, Bakochi A, Bahonjic E, Etholm L, Ekdahl CT. Alterations in Brain Inflammation, Synaptic Proteins, and Adult Hippocampal Neurogenesis during Epileptogenesis in Mice Lacking Synapsin2. *PLoS One*. 2015;10(7):e0132366. doi:10.1371/journal.pone.0132366
7. Hou Y, Chen Z, Wang L, et al. Characterization of Immune-Related Genes and Immune Infiltration Features in Epilepsy by Multi-Transcriptome Data. *J Inflamm Res*. 2022;15:2855–2876. doi:10.2147/JIR.S360743
8. Klement W, Blaquiere M, Zub E, et al. A pericyte-glia scarring develops at the leaky capillaries in the hippocampus during seizure activity. *Epilepsia*. 2019;60(7):1399–1411. doi:10.1111/epi.16019
9. Morin-Brureau M, Milior G, Royer J, et al. Microglial phenotypes in the human epileptic temporal lobe. *Brain*. 2018;141(12):3343–3360. doi:10.1093/brain/awy276
10. Pitkänen A, Lukasiuk K, Dudek FE, Staley KJ. Epileptogenesis. *Cold Spring Harbor Perspect Med*. 2015;5(10):a022822. doi:10.1101/cshperspect.a022822

11. Benson MJ, Manzanero S, Borges K. Complex alterations in microglial M1/M2 markers during the development of epilepsy in two mouse models. *Epilepsia*. 2015;56(6):895–905. doi:10.1111/epi.12960
12. Han T, Qin Y, Mou C, Wang M, Jiang M, Liu B. Seizure induced synaptic plasticity alteration in hippocampus is mediated by IL-1β receptor through PI3K/Akt pathway. *Am J Transl Res*. 2016;8(10):4499–4509.
13. Scorza CA, Marques MJG, Gomes da Silva S, Naffah-Mazzacoratti MDG, Scorza FA, Cavalheiro EA. Status epilepticus does not induce acute brain inflammatory response in the Amazon rodent Proechimys, an animal model resistant to epileptogenesis. *Neurosci Lett*. 2018;668:169–173. doi:10.1016/j.neulet.2017.02.049
14. Mosser DM, Edwards JP. Exploring the full spectrum of macrophage activation. *Nat Rev Immunol*. 2008;8(12):958–969. doi:10.1038/nri2448
15. Feng B, Tang Y, Chen B, et al. Transient increase of interleukin-1beta after prolonged febrile seizures promotes adult epileptogenesis through long-lasting upregulating endocannabinoid signaling. *Sci Rep*. 2016;6(1):21931. doi:10.1038/srep21931
16. Sun Y, Ma J, Li D, et al. Interleukin-10 inhibits interleukin-1beta production and inflammasome activation of microglia in epileptic seizures. *J Neuroinflammation*. 2019;16(1):66. doi:10.1186/s12974-019-1452-1
17. Therajaran P, Hamilton JA, TJ O, Jones NC, Ali I. Microglial polarization in posttraumatic epilepsy: potential mechanism and treatment opportunity. *Epilepsia*. 2020;61(2):203–215. doi:10.1111/epi.16424
18. Heneka MT, McManus RM, Latz E. Inflammasome signalling in brain function and neurodegenerative disease. *Nat Rev Neurosci*. 2018;19(10):610–621. doi:10.1038/s41583-018-0055-7
19. He Y, Hara H, Nunez G. Mechanism and Regulation of NLRP3 Inflammasome Activation. *Trends Biochem Sci*. 2016;41(12):1012–1021. doi:10.1016/j.tibs.2016.09.002
20. Yue J, Wei YJ, Yang XL, Liu SY, Yang H, Zhang CQ. NLRP3 inflammasome and endoplasmic reticulum stress in the epileptogenic zone in temporal lobe epilepsy: molecular insights into their interdependence. *Neuropathol Appl Neurobiol*. 2020;46(7):770–785. doi:10.1111/nan.12621
21. Meng XF, Tan L, Meng-Shan T, et al. Inhibition of the NLRP3 inflammasome provides neuroprotection in rats following amygdala kindling-induced status epilepticus. *J Neuroinflammation*. 2014;11(212). doi:10.1186/s12974-014-0212-5.
22. Rong S, Wan D, Fan Y, et al. Amentoflavone Affects Epileptogenesis and Exerts Neuroprotective Effects by Inhibiting NLRP3 Inflammasome. *Front Pharmacol*. 2019;10:856. doi:10.3389/fphar.2019.00856
23. Racine RJ. Modification of seizure activity by electrical stimulation. II. Motor seizure. *Electroencephalogr Clin Neurophysiol*. 1972;32(3):281–294. doi:10.1016/0013-4694(72)90177-0
24. Wang L, Shen J, Cai X-T, et al. Ventrolateral Periaqueductal Gray Matter Neurochemical Lesion Facilitates Epileptogenesis and Enhances Pain Sensitivity in Epileptic Rats. *Neuroscience*. 2019;411:105–118. doi:10.1016/j.neuroscience.2019.05.027
25. Socala K, Nieoczym D, Pierog M, et al. Effect of Tadalafil on Seizure Threshold and Activity of Antiepileptic Drugs in Three Acute Seizure Tests in Mice. *Neurotox Res*. 2018;34(3):333–346. doi:10.1007/s12640-018-9876-4
26. Kimball AW, Burnett WT, Doherty DG. Chemical protection against ionizing radiation. I. Sampling methods for screening compounds in radiation protection studies with mice. *Radiat Res*. 1957;7(1):1–12. doi:10.2307/3570549
27. Tzeng TC, Hasegawa Y, Iguchi R, et al. Inflammasome-derived cytokine IL18 suppresses amyloid-induced seizures in Alzheimer-prone mice. *Proc Natl Acad Sci U S A*. 2018;115(36):9002–9007. doi:10.1073/pnas.1801802115
28. Paxinos G, Franklin KBJ. *The mouse Brain in Stereotaxic Coordinates*. 2nd ed. New York: Academic Press; 2001.
29. Chu PC, Yu HY, Lee CC, Fisher R, Liu HL. Pulsed-Focused Ultrasound Provides Long-Term Suppression of Epileptiform Bursts in the Kainic Acid-Induced Epilepsy Rat Model. *Neurotherapeutics*. 2022;19(4):1368–1380. doi:10.1007/s13311-022-01250-7
30. Vezzani A, Granata T. Brain inflammation in epilepsy: experimental and clinical evidence. *Epilepsia*. 2005;46(11):1724–1743. doi:10.1111/j.1528-1167.2005.00298.x
31. Hu H, Zhu T, Gong L, et al. Transient receptor potential melastatin 2 contributes to neuroinflammation and negatively regulates cognitive outcomes in a pilocarpine-induced mouse model of epilepsy. *Int Immunopharmacol*. 2020;87:106824.
32. Perry VH, Nicoll JA, Holmes C. Microglia in neurodegenerative disease. *Nat Rev Neurol*. 2010;6(4):193–201. doi:10.1038/nrneurol.2010.17
33. Steinborn B, Zarowski M, Winczewska-Wiktor A, Wojcicka M, Mlodzikowska-Albrecht J, Losy J. Concentration of Il-1beta, Il-2, Il-6, TNFalpha in the blood serum in children with generalized epilepsy treated by valproate. *Pharmacol Rep*. 2014;66(6):972–975. doi:10.1016/j.pharep.2014.06.005
34. Li X, Han X, Bao J, et al. Nicotine increases eclampsia-like seizure threshold and attenuates microglial activity in rat hippocampus through the alpha7 nicotinic acetylcholine receptor. *Brain Res*. 2016;1642:487–496. doi:10.1016/j.brainres.2016.04.043
35. Leal B, Chaves J, Carvalho C, et al. Brain expression of inflammatory mediators in Mesial Temporal Lobe Epilepsy patients. *J Neuroimmunol*. 2017;313:82–88. doi:10.1016/j.jneuroim.2017.10.014
36. Zhang H, Yu S, Xia L, Peng X, Wang S, Yao B. NLRP3 Inflammasome Activation Enhances ADK Expression to Accelerate Epilepsy in Mice. *Neurochem Res*. 2022;47(3):713–722. doi:10.1007/s11064-021-03479-8
37. Mazarati AM, Lewis ML, Pittman QJ. Neurobehavioral comorbidities of epilepsy: role of inflammation. *Epilepsia*. 2017;58(3):48–56. doi:10.1111/epi.13786
38. Jin X, Liu MY, Zhang DF, et al. Baicalin mitigates cognitive impairment and protects neurons from microglia-mediated neuroinflammation via suppressing NLRP3 inflammasomes and TLR4/NF-kappaB signaling pathway. *CNS Neurosci Ther*. 2019;25(5):575–590. doi:10.1111/cns.13086
39. Swanson KV, Deng M, Ting JP. The NLRP3 inflammasome: molecular activation and regulation to therapeutics. *Nat Rev Immunol*. 2019;19(8):477–489. doi:10.1038/s41577-019-0165-0
40. Yuen AWC, Keezer MR, Sander JW. Epilepsy is a neurological and a systemic disorder. *Epilepsy Behav*. 2018;78:57–61. doi:10.1016/j.yebeh.2017.10.010
41. Patel DC, Tewari BP, Chaunsali L, Sontheimer H. Neuron-glia interactions in the pathophysiology of epilepsy. *Nat Rev Neurosci*. 2019;20(5):282–297. doi:10.1038/s41583-019-0126-4
42. Ekdahl CT, Claasen JH, Bonde S, Kokaia Z, Lindvall O. Inflammation is detrimental for neurogenesis in adult brain. *Proc Natl Acad Sci U S A*. 2003;100(23):13632–13637. doi:10.1073/pnas.2234031100